

CELLULAR ANALYSIS OF THE SCS7 KNOCKOUT STRAIN UNDER 5-HYDROXYMETHYLFURFURAL STRESS IN *SACCHAROMYCES CEREVISIAE*

XIAO, X. M.^{1,2#} – MOU, B. R.^{1#} – WANG, H. Y.^{1,2} – LU, F. J.¹ – LI, Q.^{1,3} – ZHAO, L.⁴ – FU, C.^{1,2} –
LONG, W. C.^{1,2} – LAI, J. F.¹ – LI, C. H.⁵ – WU, W.⁵ – MA, M. G.³ – YANG, Y. J.^{1,2*}

¹*College of Life Science, Leshan Normal University, Leshan, Sichuan 614000, China*

²*Bamboo Diseases and Pests Control and Resources Development Key Laboratory of Sichuan Province, College of Life Science, Leshan Normal University, Leshan, Sichuan 614000, China*

³*Department of Applied Microbiology, College of Resources, Sichuan Agricultural University, Wenjiang, Chengdu, Sichuan 611130, China*

⁴*Jiangxi Forestry Science and Technology Promotion and Publicity Education Center, Lanchang, Jiangxi 330000, China*

⁵*Leshan Institute of Product Quality Supervision and Testing, Leshan, Sichuan 614000, China*

[#]*These authors contributed equally*

^{*}*Corresponding author*

e-mail: rsyyj@126.com; phone: +86-187-8457-4091

(Received 3rd Jan 2025; accepted 14th Apr 2025)

Abstract. 5-hydroxymethylfurfural (HMF) is a recognized indicator of non-enzymatic browning and deterioration produced by excessive heating or storage of foods, but HMF can be converted by sulfotransferase (SULT) into 5-sulfooxymethylfurfural (SMF), a compound that harms human skeletal muscle, kidneys and other organs. Therefore, exploring the underlying HMF tolerance mechanisms in organisms is important for in protecting the human body from the harm. In our previous studies that the candidate genes *GUP1*, *SCS7*, *LAS21* and *ORM1* in the membrane fluidity pathway may be associated with HMF tolerance in *S. cerevisiae*. In this study, based on the spot-plate test, it was found that the *SCS7* gene knockout strain was found to be sensitive in 60 mM HMF. According to the subcellular structure observation, after 3 h of HMF treatment, the proportion of cells with endoplasmic reticulum (ER) damage, mitochondrial damage, and reactive oxygen species (ROS) accumulation in the *SCS7* gene knockout strain increased by 64.61%, 11.68%, and 15.87%, respectively, compared with the standard strain BY4741. In summary, gene *SCS7* promotes the stability of ER and mitochondria structure and the clearance of ROS in cells, providing guidance for the protection and treatment of organisms exposed to HMF.

Keywords: *Saccharomyces cerevisiae*, *SCS7*, 5-hydroxymethylfurfural, tolerance

Introduction

Food processing, such as heating, fermentation, and storage, can generate undesirable toxic substances, including furfural and its derivative, 5-hydroxymethylfurfural (HMF) (Martins et al., 2022). As products of the Li reaction and caramelization occurring during and long storage (Li et al., 2022; Shapla et al., 2018), they are ubiquitous in a wide range of food products, such as dried fruit, juice, caramel products, coffee, baked goods, malt and vinegar. Hence, HMF concentration has been widely recognized as a parameter affecting food browning and freshness (Salis et al., 2021). Yet the amount of brown substances and aroma compounds rises with the

increase of HMF, which add more flavor and aroma to food (Albouchi and Murkovic, 2019). In addition, furfural and furfural derivatives have also been detected in cigarette smoke and chewing tobacco (Farag et al., 2020). Numerous researchers have discovered that 5-hydroxymethylfurfural, to a certain extent, causes irritation in human eye mucosa and upper respiratory tract mucosa. It also causes human striated muscle paralysis, visceral damage and toxic side effects on genes and nerves (Xu et al., 2023). In severe cases exposure to HMF leads to gene mutation and DNA chain breaks, which increase the risk of cancer (Zhuang et al., 2025). The main reason is that 5-hydroxymethylfurfural is also a good substrate for sulfotransferases (SULTs) and HMF might be converted to a number of toxic substances including 5-sulfooxymethylfurfural (SMF) in vitro and in vivo, which can irritate the skin mucosa and eyes and harm skeletal muscle, the kidney and other body organs. The German Institute of Human Nutrition determined that the safe daily intake of furfural and furfural derivatives ranges between 4 to 30 mg per person based on human sulfotransferase on the biological conversion activity of furfural and furfural derivatives (Sachse et al., 2016). However, it was discovered that the average daily consumption of furfural and furfural derivatives is actually well above the recommended intake range, especially for 5-hydroxymethylfurfural, reaching 30 – 150 mg per day (Liu et al., 2023).

5-hydroxymethylfurfural is an endogenous contaminant widely present in food that is potentially toxic and highly exposed in the diet, yet there is no reliable scavenging mechanism to reduce 5-hydroxymethylfurfural levels and its toxicity in food production. Therefore, reducing levels of 5-hydroxymethylfurfural in foods and further reducing the health risks to consumers have become important trends in food safety. At present, ultraviolet technology, vacuum technology, microbial and other methods are often used to degrade 5-hydroxymethylfurfural in food. For example, because of its low boiling point, vacuum technology is applied to effectively reduce HMF content especially in coffee preservation (Park et al., 2021), but the technology is mainly suitable for foods with low water activity (Monsalve-Atencio et al., 2023); ultraviolet irradiation has been used to treat food to mitigate the formation of 5-hydroxymethylfurfural produced by thermal processing (Barut Gok et al., 2024); in addition, yeast fermentation can effectively eliminate 5-hydroxymethylfurfural in foods, which Akillioglu attributed to yeast cells' ability to convert 5-hydroxymethylfurfural in the substrate to 5-hydroxymethylfurfural during fermentation and this technology has been widely applied in the processing of instant coffee and wort (Akillioglu et al., 2011). Besides, some fungi, such as the filamentous fungus *Amorphotheca resinae* ZN1, have been found to facilitate the conversion of 5-hydroxymethylfurfural to hydroxymethylfurfuryl alcohol or hydroxymethylfurfuric acid during fermentation (Ran et al., 2014).

The advantage of biological 5-hydroxymethylfurfural degradation is that toxic byproducts are completely converted. Nevertheless, low degradation efficiency restricts the wide application of biodegradation method (Vina-Gonzalez et al., 2020). Thus, obtaining a microbial strain that can efficiently degrade 5-hydroxymethylfurfural is the key to the problem. *S. cerevisiae*, a model organism, is commonly used in industrial fermentation because of its easy genomic manipulation and its close relatedness to higher eukaryotes (Santos et al., 2025), and 5-hydroxymethylfurfural is toxic to *S. cerevisiae*, interfering with the normal expression of key enzymes involved in cellular metabolism, which in turn affects the cell growth and development and fermentation efficiency (Soares et al., 2021). In this paper, we used 5-hydroxymethylfurfural to treat

the whole gene knockout strain of *S. cerevisiae*, screened out the key genes *GUPI*, *SCS7*, *LAS21* and *ORM1* as potential genes for tolerance to 5-hydroxymethylfurfural in *S. cerevisiae* enriched in the membrane mobility pathway, and validated their phenotypes. All these efforts are providing reference and guidance for transformation into highly tolerant *S. cerevisiae* strains.

Experimental materials and methods

Test materials

The non-essential gene knockout strain bank of *S. cerevisiae* used in this study was donated by Professor Beidong Liu of the University of Gothenburg. 5-hydroxymethylfurfural (abbreviation: HMF), peptone, AGAR, glucose, Genomyc in (G418), yeast extraction powder, sodium chloride and other strains were purchased from Chengdu Vanke Co, LTD.

Fluorescent staining agent: Diaminophenylindole (DAPI) are purchased from Shanghai, China, 2',7'-dichlorofluorescein diacetate from Sigma, Mito Tracker Green FM, Yeast Vacuole Membrane Marker MDY-64 and ER-Tracker Red dye all from Thermo Scientific company.

Test methods

Enrichment of membrane fluidity pathway and functional analysis of related genes

In the preliminary laboratory study, a set of over 4400 gene knockout strains of brewing yeast were inoculated onto agar plates containing 5-hydroxymethylfurfural (HMF), and the half-maximum inhibitory concentration of HMF was determined to be 60 mM (Li et al., 2023). Analysis of the Images of the control and experimental plates were quantitatively analyzed using the SGAtools and genes related to the HMF stress response were screened (*Table A1*). Screening weights of ≥ 0.2 or ≤ -0.2 were used as criteria to determine the strains tolerant or sensitive to HM, which is based on previous experiments and literature review (Li et al., 2023). Using these criteria, 202 HMF-sensitive knockout candidates and 92 HMF-tolerant candidates were screened. KEGG and GO enrichment analysis were conducted to further investigate the 92 tolerance genes employing the Cytoscape (Shannon et al., 2003). These genes were found to be primarily involved in multiple aspects of cellular metabolism, including membrane fluidity, the INO-80 complex, intracellular transport regulation, and protein phosphorylation. Due to the vast number of pathways involved, this study mainly focuses on the relevant genes acting upon the membrane fluidity pathways, where four genes - *GUPI*, *SCS7*, *LAS21*, and *ORM1* - were significantly enriched. Consequently, this experiment aims to conduct in-depth phenotypic studies on these four genes enriched in the membrane fluidity pathway, and elucidate their specific mechanisms mediating the action in response to HMF stress in the brewing yeast.

Spot test verification

The preparation of YPD Medium involved combining 10 g of yeast extract, 20 g of glucose, 20 g of peptone, and 1000 mL of distilled water (for solid medium, an additional 20 g of AGAR was added). For the YPD + G418 Liquid Medium, G418 was added at a

concentration of 100 mg/L to the already prepared YPD medium. Subsequently, the strain was inoculated onto a YPD + G418 plate and streaked for isolation to obtain single colonies. These single colonies were then transferred into a 100 mL Erlenmeyer flask containing 30 mL of YPD + G418 liquid medium, and incubated with shaking at 30° C and 200 r/min for 18-24 h. The cell concentration (OD₆₀₀) of the cultured broth was adjusted to 1.0, followed by performing serial 10-fold dilutions. Using a multichannel pipette, the diluted cultures were dispensed onto YPD + G418 solid media containing various concentrations of inhibitors. The plates were labeled and incubated at 30° C for 3-4 days before being observed and photographed.

Observation of subcellular structure

(1) Standard strain *BY4741* and the *SCS7* knockout strain were respectively cultured in liquid medium YPD + G418 (final concentration of G418 was 100 mg/L) at 30°C and in a constant temperature shaker (200 r/min) for 8-12 h.

(2) The bacteria solution with a spectrophotometric value (OD₆₀₀) of 0.8 was cultured in a constant temperature shaker for 0 h and 3 h. 0 h was taken as pre-treatment and 3 h as post-treatment (after treatment: HMF inhibitor was added to the culture medium for culture).

(3) Subcellular structure was observed after culture. Dyes 2'7'-DCFdiacetate, Mito Tracker Green FM, Vacuole Membrane Marker MDY-64, diaminophenylindole (DAPI) and ER-Tracker Red (thawed in advance) were mixed into centrifuged bacterial solution, followed by ROS staining for 2 h, nuclear staining for 17 min, mitochondrial staining for 45 min, endoplasmic reticulum staining for 1.5 h and vacuole staining for 5 min. Finally, we observed the integrity of cellular ultrastructure evaluated accumulation of ROS, disorganization of nuclear chromatin, mitochondrial membrane damage, endoplasmic reticulum damage, and vacuolar membrane damage using fluorescence microscopy equipped with filters for DIC, GFP, Rhod and DAPI. We counted the cells of *BY4741* standard strain and gene knockout strain from different solution in the field of view (at least 100 cells) and calculated the percentages of positive ROS cells and damaged organelles.

Statistical method and the applied software

In the experiment, the average of the three-sample data is utilized, and the disparities among the samples are examined using a T-test. Specifically, in the T-test, asterisks (*) denote a significant difference ($p < 0.05$), double asterisks (**) signify a very significant difference ($p < 0.01$), and triple asterisks (***) indicate an extremely significant difference ($p < 0.001$). Primarily, Graphpad Prism 8 software was employed for graphing and statistical analysis of the data in this experiment.

Results and analysis

Cytoplasmic vesicles pathway enriched genes and their sensitivity or tolerance screening and function

Screening and function of membrane fluidity pathway genes and sensitive or tolerant genes KEGG and GO enrichment analysis on differentially phenotypic genes using Cytoscape software revealed that *GUP1*, *SCS7*, *LAS21* and *ORM1* genes enriched on

membrane fluidity pathway showed tolerance to HMF (see *Table 1* and the *Appendix*). The screening scores of these four tolerance genes in the membrane fluidity pathway were -0.30, -0.45, -0.25 and -0.26, respectively. As shown in *Figure 1*, *GUP1* and plasma membrane proteins were involved in the remodeling of GPI-anchored proteins. *SCS7* determines the cytochrome b5-like domains and the hydroxylase or desaturase domains during the α -hydroxylation of sphingolipid-related long-chain fatty acids; *LAS21* is involved in the biosynthesis of glycosylphosphatidylinositol (GPI) core structure, catalyzing the addition of side chain ethanolamine phosphate to α -1,6-linked second mannose residues of the GPI lipid precursors, and also determines the composition of endoplasmic reticulum and mutations that affect cell wall integrity; *ORM1* controls proteins that are key regulators of sphingolipid homeostasis, in which Orm1p and Orm2p control membrane biogenesis by coordinating lipid homeostasis and protein quality control.

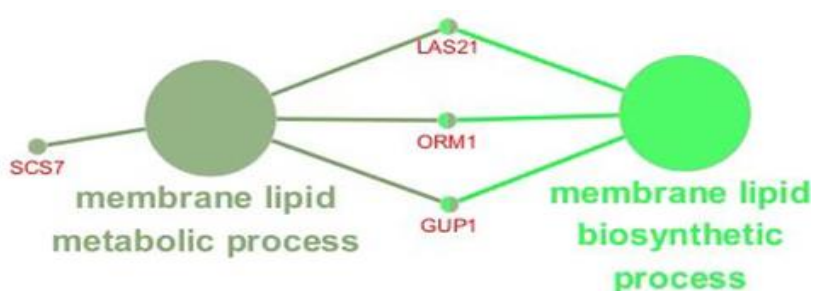


Figure 1. KEGG enrichment analysis of genes related to HMF tolerance on membrane fluidity pathway

Table 1. Key genes of membrane fluidity pathway to HMF tolerance

NO	AN	AO	NC size (EX)	NC std. (EX)	NC size (CN)	NC std. dev. (CN)	Score	Score std.	P-Value
1	<i>GUP1</i>	<i>YGL084C</i>	0.51	0.00	0.81	0.00	-0.30	0.00	0.00
2	<i>SCS7</i>	<i>YMR272C</i>	0.61	0.07	1.06	0.02	-0.45	0.07	0.00
3	<i>LAS21</i>	<i>YJL062W</i>	0.74	0.01	0.99	0.01	-0.25	0.02	0.00
4	<i>ORM1</i>	<i>YGR038W</i>	0.93	0.01	1.20	0.03	-0.26	0.01	0.00

NO: Number; AO: Array ORF; AN: Array Name; NC size: Normalized colony size; NC std.: Normalized colony std. dev.; EX: Experiment; CN: Control

Spot test verification

In this experiment, we took advantage of the toxic properties of 5-hydroxymethylfurfural (HMF), a representative inhibitor of furan substances, to screen the membrane fluidity pathway tolerance genes. Since the general screening table is only a preliminary screening of tolerant or sensitive genes, a spot test verification will be performed for final verification. The final inhibition concentration was determined to be 60 mM as a result of a series of trial on concentration in pre-lab. As shown in *Figure 2*, after a serial ten-fold dilution, each diluent of BY4741 standard strain (CK) and *GUP1* knockout strain, the *SCS7*

knockout strain, *LAS21* knockout strain and *ORM1* knockout strain was plated on solid medium YPD + G418 without HMF and YPD + G418 with 60 mM HMF, respectively. Three replicates were set for each strain. On YPD + G418 solid medium, five colonies of each of the five strains grew, indicating that there was no significant difference in the growth of these five strains with the absence of HMF. Standard strain BY4741, *GUP1* knockout strain, *LAS21* knockout strain and *ORM1* knockout strain were cultured at the same time on the plates containing 60 mM HMF, where only 3 colonies arose on plates of *BY4741* standard strain, *GUP1* knockout strain, *LAS21* knockout strain and *ORM1* knockout strain, and there was no significant difference between their growth. On the plates of *BY4741* standard strain and *SCS7* gene knockout strain cultured at the same time, 3-4 colonies grew out of *BY4741* standard strain, while only grew 1 colony grew out of *SCS7* gene knockout strain, which clearly shows that *SCS7* gene knockout strain is less tolerant to HMF. Given that, *SCS7* gene will be further verified in future study.

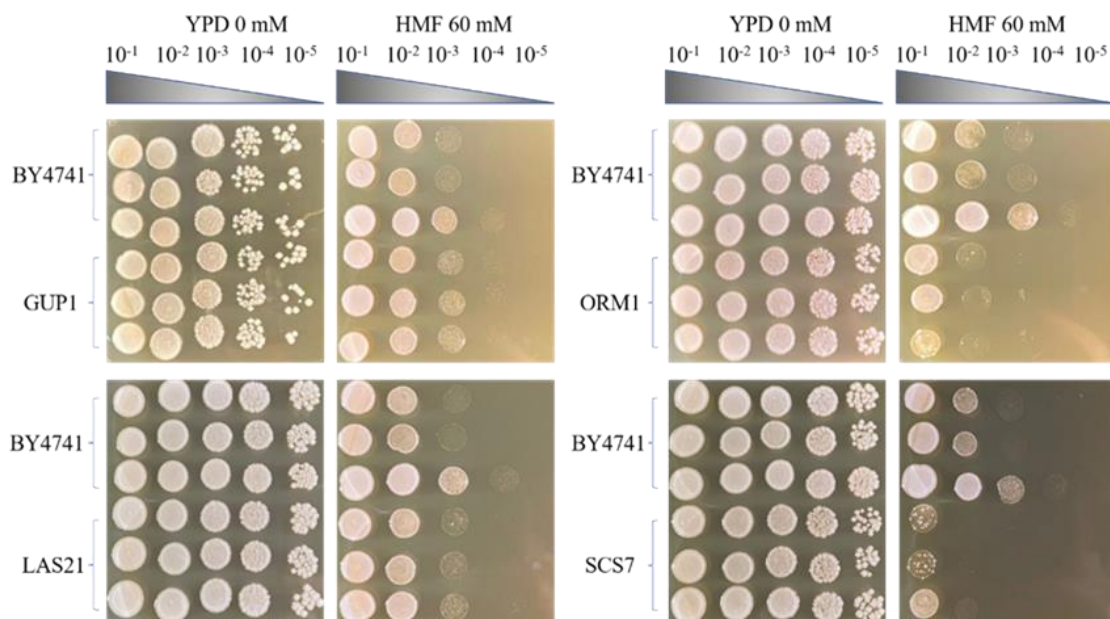


Figure 2. Spot-test verification of candidate genes

Subcellular structure observation test

Reactive oxygen species

As shown in *Figure 3A*, cells presented different morphologies with different levels of reactive oxygen species (ROS) in cells; When ROS accumulated in cells, cells showed green fluorescence signal of reactive oxygen species after staining with 2',7'-DCF diacetate dye. If there was no accumulation of ROS in the cells, no green signal was detected under the fluorescence microscope. As shown in *Figure 3B*, after HMF treatment for 0 h and 3 h, 22.48% and 22.26% of ROS-containing cells were detected respectively, indicating that HMF does not affect reactive oxygen levels in *BY4741*. At 0 h and 3 h, 22.52% and 38.13% of *SCS7* gene knockout strain cells showed the presence of reactive oxygen species, respectively, suggesting that HMF would facilitate the accumulation of reactive oxygen species in cells after *SCS7* gene knockout.

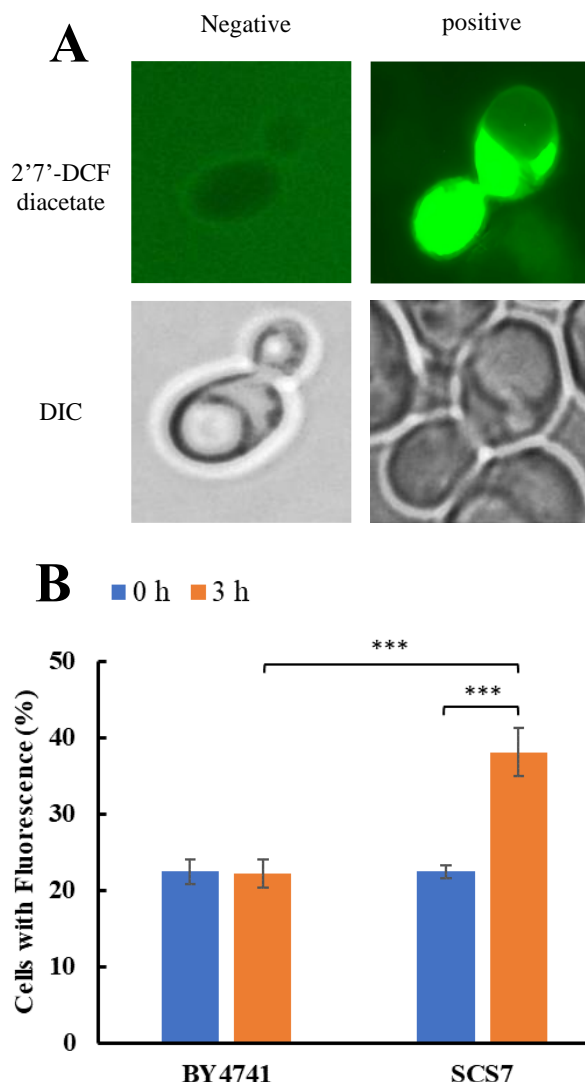


Figure 3. Proportion of cells containing ROS of different strains under non-stop treatment. (A) accumulation of reactive oxygen species in cells. (B) the proportion of cells that contained reactive oxygen species after 0 mM and 60 mM HMF treatment for 0 and 3 h. 2'7'-DCF diacetate (top column): reactive oxygen species indicator dye. DIC (down column): differential interference microscope. *** $p < 0.001$ indicates significant differences (T-test). The data represent averages of three experiments. At least 100 cells were examined on each bright-field image

Mitochondria

As shown in *Figure 4A*, the mitochondria of *S. cerevisiae* showed different levels of damage (normal and abnormal) with the presence of 60 mM HMF. After staining with Mito Tracker Green FM stain, different cellular damages could be observed under fluorescence. As shown in *Figure 4B*, the percentages of cells with mitochondrial damage at 0 h were 8.93% for BY4741 standard strain and 12.90% for the SCS7 knockout strain. However, after 0 mM HMF treatment for 3 h, the shares rose to 10.95% and 22.63%, respectively. By analyzing these data, we can see that the SCS7 gene plays a key role in maintaining the mitochondrial morphology in yeast cells.

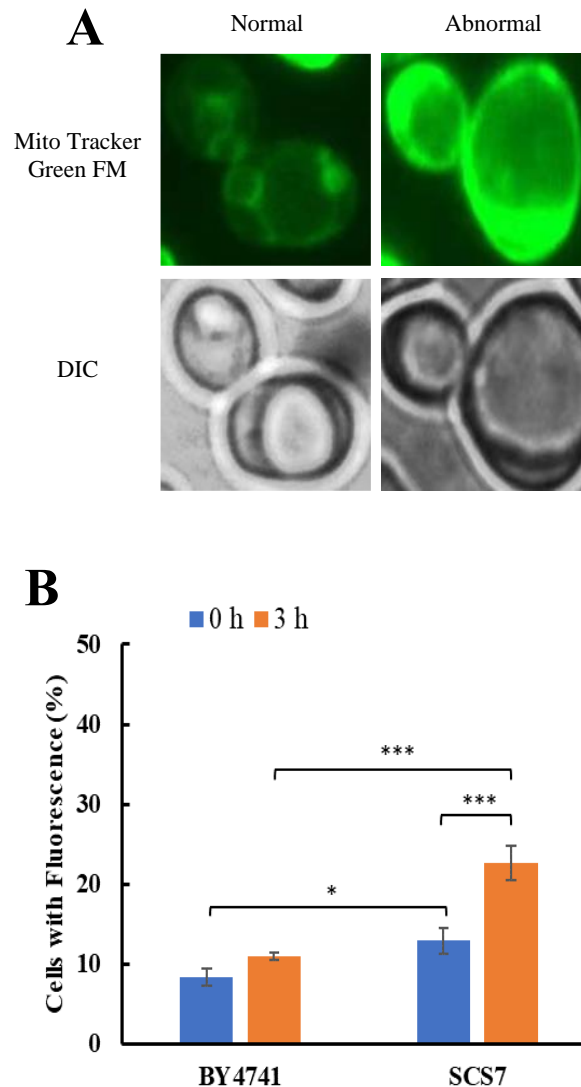


Figure 4. Mitochondrial morphological changes in *Saccharomyces cerevisiae*. (A) different morphology of mitochondria in cells. (B) the proportion of cells that displayed abnormal mitochondria after 0 mM and 60 mM HMF treatment for 0 and 3 h. Mito Tracker Green FM (top column): the mitochondria-specific dye. DIC (down column): differential interference microscope. * $p < 0.05$; *** $p < 0.001$ indicates significant differences (T-test). The data represent averages of three experiments. At least 100 cells were examined on each bright-field image

Endoplasmic reticulum

As shown in Figure 5A, we divided the structural morphology of the endoplasmic reticulum in living cells was divided into two categories - normal and abnormal for the convenience of subsequent statistics. As seen from Figure 5B, the percentages of cells with endoplasmic reticulum damage were 11.3% for BY4741 standard strain and 10.56% for the SCS7 knockout strain at 0 h, respectively, which imply that a mild difference in their damage degrees. However, after being treated with 60 mM HMF for 3 h, two strains vary dramatically in their change of ER damage; the proportion of cells with damaged ER in BY4741 was 17.32%, showing a mild increase of 6.02%, whereas, the figure for SCS7 gene knockout strain was 81.93%, representing a hike of 71.37%.

We can conclude from these figures that HMF destroys the structure of the endoplasmic reticulum of the strains, and has a more negative effect on strains with *SCS7* gene knocked out.

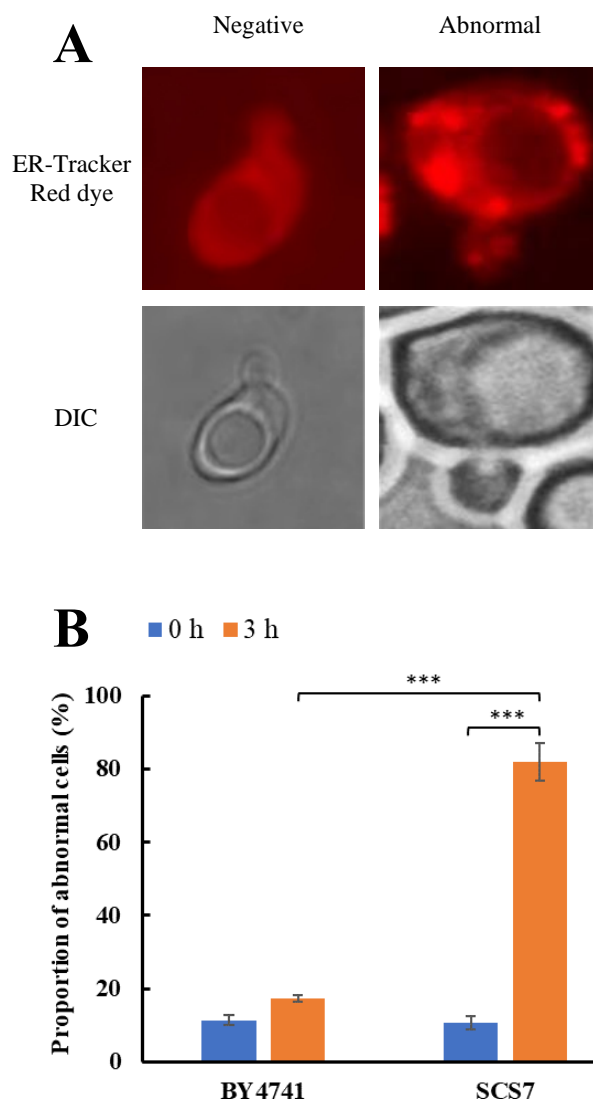


Figure 5. Morphological changes of endoplasmic reticulum in *Saccharomyces cerevisiae*. (A) different morphologies of the ER in cells. (B) the proportion of cells that displayed abnormal ER after 0 mM and 60 mM HMF treatment for 0 and 3 h. ER-Tracker Red dye (top column): endoplasmic reticulum specific dye. DIC (down column): differential interference microscope. *** $p < 0.001$ indicates significant differences (T-test). The data represent averages of three experiments. At least 100 cells were examined on each bright-field image

Vacuoles

As shown in Figure 6A, after being treated by HMF and stained with Vacuole Membrane Marker MDY-64 stain, cell vacuoles in this test presented two states: single large vacuole and two (or more) small vacuoles which indicate abnormal cells (damaged cells). It shows a slight difference of the proportion of cells with vacuole damage in standard strain BY4741 after being exposed to 60 mM HMF for 3 h,

registering a modest rise from 20.10% to 20.59% in *Figure 6B*. As for *SCS7* gene knockout strain, the percentages at 0 h and 3 h were 22% and 24.93%, respectively, which shows an unremarkable effect of HMF and therefore supports our conclusion that intracellular vacuole structure of *SCS7* strain maintains stable under HMF stress.

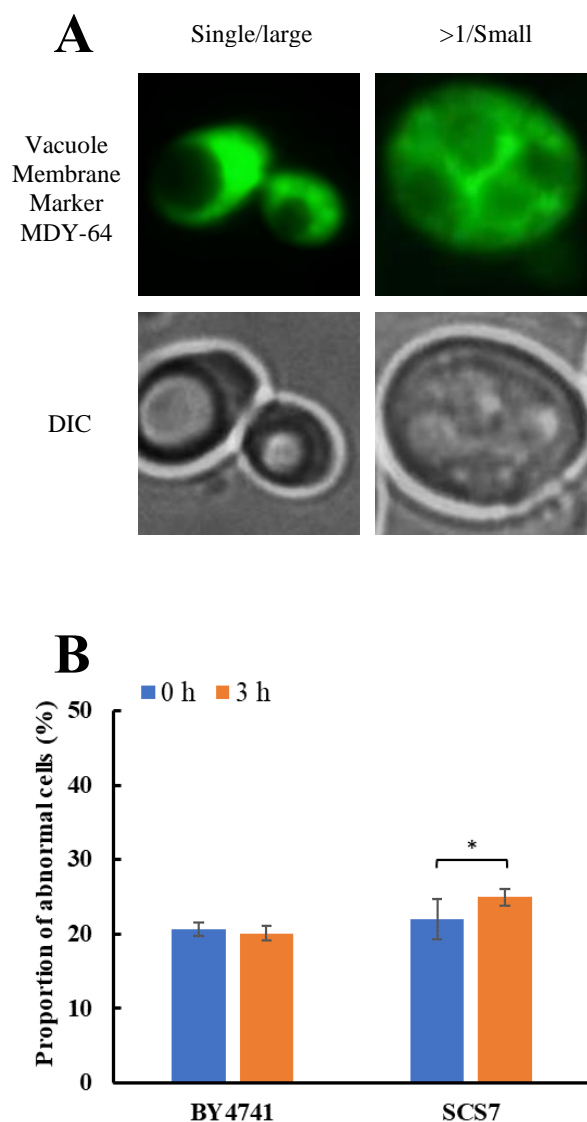


Figure 6. Morphological changes of vacuoles in *Saccharomyces cerevisiae*. (A) different morphology of vacuoles in cells. (B) the proportion of cells that displayed abnormal vacuole after 0 mM and 60 mM HMF treatment for 0 and 3 h. Vacuole Membrane Marker MDY-64 (top column): vacuole specific dye. DIC (down column): differential interference microscope. Single/large: single large vacuole. > 1/Small: more than single small vacuole. * $p < 0.05$ indicates significant differences (T-test). The data represent averages of three experiments. At least 100 cells were examined on each bright-field image

Chromatin

As shown in *Figure 7B*, the normal chromatin structure in the cell is small and compact. However, under HMF stress, the chromatin structure becomes abnormal and diffuses in all directions. As seen in *Figure 7B*, BY4741 the percentages of cells with

abnormal chromatin at 0 h and 3 h for standard strain were 1.17% and 1.66%, respectively, and the figures for the *SCS7* knockout strain were 2.27% and 1.77%, all below 3%. Thus, we concluded that 60 mM HMF basically did not damage the chromatin in *S. cerevisiae*.

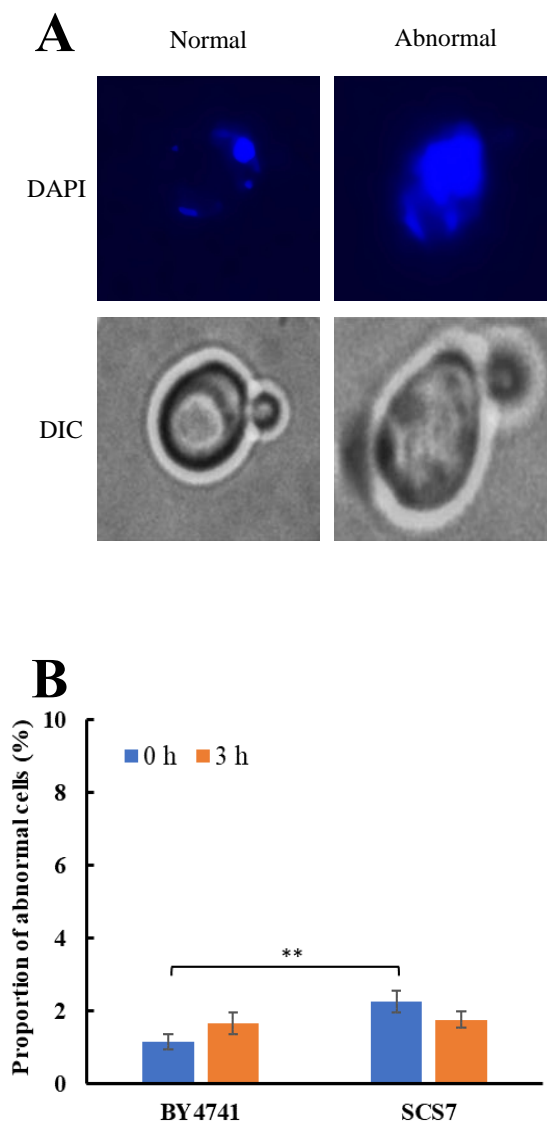


Figure 7. Morphological changes of chromatin in *Saccharomyces cerevisiae*. (A) different morphologies of chromatin in cells. (B) the proportion of cells that displayed abnormal chromatin after 0 mM and 60 mM HMF treatment for 0 and 3 h. Diaminophenylindole (DAPI) (top column): DNA specific dye. DIC (down column): differential interference microscope. ** $p < 0.01$ indicates significant differences (T-test). The data represent averages of three experiments. At least 100 cells were examined on each bright-field image

Discussion and conclusion

In this experiment, enrichment analysis revealed that four key genes involved in the membrane fluidity pathway—*GUP1*, *SCS7*, *LAS21*, and *ORM1*—were associated with HMF tolerance and they were identified as downregulated genes in the initial screen of SGA database. In prior research, which relied heavily on transcriptome, the identified

genes associated with HMF tolerance were mainly enriched in pathways such as plasma membrane, cellular protein degradation metabolism, metabolic processes of cellular amino acids and their derivatives, DNA metabolism, and hydrolytic enzyme activity (Donoso et al., 2021). However, this study creatively used phenotype validation and identified novel HMF tolerance genes that were enriched in membrane fluidity.

One of the tolerance genes discovered in our plaque assay is *ORM1*, which encodes the protein Orm1p. Orm1p is an endoplasmic reticulum resident protein that plays an essential role in sphingolipid metabolism and proteostasis of brewing yeast (Mathivanan and Nachiappan, 2023) as well as maintaining the structural integrity of V-ATPase (Breslow et al., 2010). V-ATPase is a multi-subunit complex responsible for the acidification of intracellular vesicles and organelles and has active roles in diverse cellular functions, including vesicle transport, endocytosis, and membrane fusion (Hooper et al., 2022; Seidel, 2022; Sun et al., 2023). The study conducted by Tani and Toume (2015) further corroborates that the absence of the *ORM1* gene leads to a decrease in V-ATPase activity, potentially affecting vesicle transport and membrane fusion that are directly linked to the stress response. In this study, knocking out *ORM1* increased the strain's sensitivity to HMF, probably because the lack of *ORM1* caused the dysfunction of vesicle transport and membrane fusion and therefore inhibited cell growth. Notably, under the same HMF stress conditions, the growth inhibition of *SCS7* gene knockout strains was more pronounced. This suggests that *SCS7* may play a more substantial role in the stress response of brewing yeast to HMF through a tolerance mechanism distinct from Orm1p's.

Previous studies have demonstrated that membrane fluidity significantly impacts cell wall structure. Membrane proteins, as an essential component of plasma membranes, rely on membrane fluidity to perform their functions (Sastre et al., 2020; Ruiz et al., 2023). Ferraz et al. (2021) discovered that alterations in membrane fluidity can lead to changes in membrane protein conformation and function, thereby affecting various cellular physiological processes, including substance transport, cell wall synthesis, and signal transduction. Such alterations not only influence the permeability of cell membranes but may also regulate the expression of cell wall-related genes and the synthesis of cell walls through intricate signal transduction networks. Both HMF and furfural are toxic for the aldehyde groups and furan rings they carry (Liu and Ma, 2020), so the brewing yeast may share similar mechanisms in tolerance of furfural and HMF. For instance, the cell wall gene *TIR4* plays a crucial role in both furfural and HMF tolerance (Ma and Liu, 2010; Wang et al., 2023). Additionally, Wang et al. (2023) observed that mutations of cell wall-related genes including *CCW14*, *ECM30*, *FKS1*, *GAS2*, *CDA1*, and *CDA2* are associated with the tolerance of brewing yeast cells to furfural. Subsequent experiments will focus on the relationship between membrane fluidity and cell wall synthesis, elucidating the mechanism by which changes in membrane fluidity affect cell wall synthesis and, in turn, affect cell growth under HMF stress conditions.

Previous studies have demonstrated that knocking out the *SCS7* gene can enhance the tolerance of brewing yeast strains to Kahalalide F (Herrero et al., 2007) and Yilidixin (Herrero et al., 2008). However, in this study, knockout of the *SCS7* gene resulted in sensitivity of brewing yeast to HMF stress. Analysis of the chemical structure of Kahalalide F and Yilidixin revealed the main toxic groups of the two compounds are ketones and phenolic rings, respectively but in contrast, the main toxic groups of HMF are aldehyde groups and furan rings. The difference in toxic groups of the inhibitors

accounts for the distinct physiological and biochemical characteristics of the *SCS7* knockout strains. Importantly, deletion of the *SCS7* gene not only affects the drug tolerance of brewing yeast but also regulates the synthesis or metabolism of IPC-C. IPC-C, as a key component of sphingolipids, which is vital for the structure and function of brewing yeast cell membranes, its deficiency may decrease the stability of the cell membrane structure, and thereby disrupt normal cellular physiological functions (Ikeda et al., 2021; Otsu et al., 2020; Tanaka and Tani, 2018). Under HMF stress, the growth of *SCS7* gene knockout strains is inhibited, and membrane organelles such as the endoplasmic reticulum and mitochondria are damaged. Although these phenomena are likely linked to changes in IPC-C metabolism, further experiments are required to clarify the specific relationship between the absence of IPC-C and the damage to these organelles. In summary, this study has shed some light on the inextricable connection between the *SCS7* gene and HMF tolerance, which differs from previously discovered mechanisms behind sensitivity to Kahalalide F and Yilidixin. These novel findings provide a new perspective for exploring the physiological mechanisms of brewing yeast and offer directions for future research.

The Scs7p is a key membrane-bound protein that helps membranes maintain fluidity. It participates in the metabolism of inositol phosphoceramide and very long-chain fatty acids (VLCFA) and plays a crucial role in stabilizing the structure of the endoplasmic reticulum (Dunn et al., 1998). Previous studies have shown that the *SCS7* gene occupies a central position of the nucleus, and its deletion leads to a significant decrease in VLCFA hydroxylation levels (Peng et al., 2021). This suggests that Scs7p may function as a key enzyme for VLCFA hydroxylation, and depletion of *SCS7* decreases the Scs7p-catalyzed hydroxylation of the VLCFA. Since VLCFA hydroxylation plays crucial physiological and structural roles and has a profound impact on the further metabolism and utilization of fatty acids (Erdbrugger and Frohlich, 2020), knocking out *SCS7* gene would considerably decrease VLCFA hydroxylation levels, that is, VLCFA cannot be effectively hydroxylated, which will affect subsequent biological activity. Given the critical role of hydroxylated VLCFA in the structure and function of cell membranes, its reduction would make membranes less stable and fluid. The loss in stability and fluidity in turn impairs the functions that membranes perform, including cellular transport and signal transduction, resulting in a delay in cell growth. Additionally, the compromised cell membrane function may exacerbate the stress on the endoplasmic reticulum, which further compromises its normal function. Subcellular structure observations revealed that the endoplasmic reticulum damage is more severe in *SCS7* gene knockout strains, probably because HMF, upon entering the cell, reacts with lipids or proteins on the cell membrane, disrupting its structure and function. The disruption may further affect the structure and function of the endoplasmic reticulum, leading to the accumulation of endoplasmic reticulum stress. The excessive stress leads to the failure of normal synthesis of some proteins, which may include proteins on the mitochondrial membrane, such that the knockout strain suffers more severe mitochondrial damage than BY4741 does under HMF stress. Excessive mitochondrial damage well explains the occurrence of electron leakage and generation of a large amount of reactive oxygen species. In summary, *SCS7*, as a key enzyme for VLCFA hydroxylation, plays a crucial role in maintaining cell membrane structure and function, for its deficiency not only affects the metabolism and utilization of fatty acids but also weakens the cellular tolerance to stress conditions such as HMF. Furthermore, by stabilizing the endoplasmic reticulum, *SCS7* helps to alleviate endoplasmic reticulum stress, thereby safeguarding

cells from damage from stressors such as HMF. Therefore, *SCS7* is of great importance in HMF tolerance and endoplasmic reticulum protection.

In this study, we discovered that the tolerance of *S. cerevisiae* to HMF is related to membrane fluidity, which was a new from preceding studies on the HMF tolerance mechanism. Previously researchers have found that tolerance of *S. cerevisiae* to other environmental factors is correlated with membrane fluidity. For example, it was found that lower membrane fluidity leads to higher ethanol tolerance in brewer's yeast (Lairon-Peris et al., 2021). In addition, it was also revealed that regulation of membrane fluidity can be achieved by combining multiple factors including lipid composition (e.g., ratio of phosphatidylcholine (PC) to phosphatidylethanolamine (PE), fatty acid chain length and the ratio of saturated and unsaturated fatty acids, and changes in membrane proteins. This paper highlights the positive correlation between HMF tolerance and membrane fluidity Besides, previous research has found that increased membrane fluidity results in increased ethanol tolerance (Li et al., 2023). This has also been demonstrated in the study by Wu and Wang that an increasing the lipid unsaturation index by increasing unsaturated fatty acids enhances the membrane fluidity and subsequently enhances their tolerance to ethanol, cold and salt stress (Wang et al., 2024; Wu et al., 2020); in turn, reducing membrane fluidity would reduce ethanol, freezing and salt tolerance. So why can both decrease and increase in membrane fluidity improve the tolerance of *S. cerevisiae* to ethanol? It may have something to do with the proportion of fatty acids of different lengths and saturations as well (Mbuyane et al., 2021). Therefore, more research is required to explore the mechanism of HMF tolerance regulated by *SCS7* gene.

Conclusion

In this study, we adopted the creative approach of using the whole gene knockout library of *S. cerevisiae* for subcellular structure verification. Through bioinformatics analysis, we have discovered that gene *SCS7* is associated with 5-hydroxymethylfurfural tolerance; phenotypic verification through spot plate assay and subcellular structure observation confirmed the important role that gene *SCS7* plays in maintaining the structural stability of endoplasmic reticulum in the membrane fluidity pathway. All these results lay a theoretical foundation for improving the tolerance of *S. cerevisiae* strains to HMF, and contribute to lowering the cost of HMF conversion in large-scale production.

REFERENCES

- [1] Akillioglu, H. G., Mogol, B. A., Gokmen, V. (2011): Degradation of 5-hydroxymethylfurfural during yeast fermentation. – Food Addit Contam Part A Chem Anal Control Expo Risk Assess 28(12): 1629-1635.
- [2] Albouchi, A., Murkovic, M. (2019): LC method for the direct and simultaneous determination of four major furan derivatives in coffee grounds and brews. – J Sep Sci 42(9): 1695-1701.
- [3] Barut Gok, S., Yikmis, S., Levent, O., Bozgeyik, E., Ilaslan, K., Aydin, V. G. (2024): Influence of ultrasonication and UV-C processing on the functional characteristics and anticarcinogenic activity of blackthorn vinegar. – ACS Omega 9(34): 36699-36709.

- [4] Breslow, D. K., Collins, S. R., Bodenmiller, B., Aebersold, R., Simons, K., Shevchenko, A., Ejsing, C. S., Weissman, J. S. (2010): Orm family proteins mediate sphingolipid homeostasis. - *Nature* 463(7284): 1048-1053.
- [5] Donoso, R. A., Gonzalez-Toro, F., Perez-Pantoja, D. (2021): Widespread distribution of hmf genes in Proteobacteria reveals key enzymes for 5-hydroxymethylfurfural conversion. - *Comput Struct Biotechnol J* 19: 2160-2169.
- [6] Dunn, T. M., Haak, D., Monaghan, E., Beeler, T. J. (1998): Synthesis of monohydroxylated inositolphosphorylceramide (IPC-C) in *Saccharomyces cerevisiae* requires *Scs7p*, a protein with both a cytochrome b5-like domain and a hydroxylase/desaturase domain. - *Yeast* 14(4): 311-321.
- [7] Erdbrugger, P., Frohlich, F. (2020): The role of very long chain fatty acids in yeast physiology and human diseases. - *Biol Chem* 402(1): 25-38.
- [8] Farag, M. R., Alagawany, M., Bin-Jumah, M., Othman, S. I., Khafaga, A. F., Shaheen, H. M., Samak, D., Shehata, A. M., Allam, A. A., Abd El-Hack, M. E. (2020): The toxicological aspects of the heat-borne toxicant 5-hydroxymethylfurfural in animals: a review. - *Molecules* 25(8).
- [9] Ferraz, L., Sauer, M., Sousa, M. J., Branduardi, P. (2021): The plasma membrane at the cornerstone between flexibility and adaptability: implications for *saccharomyces cerevisiae* as a cell factory. - *Front Microbiol* 12: 715891.
- [10] Herrero, A., Alvarez, E. and Moreno, S. (2007): Kahalalide F antitumor activity depends on cell membrane levels of *Scs7/FA2H*-mediated sphingolipid hydroxylation. - *Cancer Research*. 67(9): 4829.
- [11] Herrero, A. B., Astudillo, A. M., Balboa, M. A., Cuevas, C., Balsinde, J., Moreno, S. (2008): Levels of *SCS7/FA2H*-mediated fatty acid 2-hydroxylation determine the sensitivity of cells to antitumor PM02734. - *Cancer Res* 68(23): 9779-9787.
- [12] Hooper, K. M., Jacquin, E., Li, T., Goodwin, J. M., Brumell, J. H., Durgan, J., Florey, O. (2022): V-ATPase is a universal regulator of LC3-associated phagocytosis and non-canonical autophagy. - *J Cell Biol* 221(6).
- [13] Ikeda, A., Hanaoka, K., Funato, K. (2021): Protocol for measuring sphingolipid metabolism in budding yeast. - *STAR Protoc* 2(2): 100412.
- [14] Lairon-Peris, M., Routledge, S. J., Linney, J. A., Alonso-Del-Real, J., Spickett, C. M., Pitt, A. R., Guillamon, J. M., Barrio, E., Goddard, A. D., Querol, A. (2021): Lipid composition analysis reveals mechanisms of ethanol tolerance in the model yeast *Saccharomyces cerevisiae*. - *Appl Environ Microbiol* 87(12): e0044021.
- [15] Li, H., Yang, F. H., Zhang, W. C., Zhang, Z. J., Yu, S. J. (2022): Effects of moisture content on the enolization products formation in glucose-proline Maillard reaction models. - *J Sci Food Agric* 102(15): 7249-7258.
- [16] Li, Q., Feng, P., Tang, H., Lu, F., Mou, B., Zhao, L., Li, N., Yang, Y., Fu, C., Long, W., Xiao, X., Li, C., Wu, W., Wang, G., Liu, B., Tang, T., Ma, M., Wang, H. (2023): Genome-wide identification of resistance genes and cellular analysis of key gene knockout strain under 5-hydroxymethylfurfural stress in *Saccharomyces cerevisiae*. - *BMC Microbiol* 23(1): 382.
- [17] Liu, Q., Zhou, P., Luo, P., Wu, P. (2023): Occurrence of furfural and its derivatives in coffee products in China and estimation of dietary intake. - *Foods* 12(1).
- [18] Liu, Z. L., Ma, M. (2020): Pathway-based signature transcriptional profiles as tolerance phenotypes for the adapted industrial yeast *Saccharomyces cerevisiae* resistant to furfural and HMF. - *Appl Microbiol Biotechnol* 104(8): 3473-3492.
- [19] Ma, M., Liu, Z. L. (2010): Comparative transcriptome profiling analyses during the lag phase uncover YAP1, PDR1, PDR3, RPN4, and HSF1 as key regulatory genes in genomic adaptation to the lignocellulose derived inhibitor HMF for *Saccharomyces cerevisiae*. - *BMC Genomics* 11: 660.

- [20] Martins, F., Alcantara, G., Silva, A. F. S., Melchert, W. R., Rocha, F. R. P. (2022): The role of 5-hydroxymethylfurfural in food and recent advances in analytical methods. - *Food Chem* 395: 133539.
- [21] Mathivanan, A., Nachiappan, V. (2023): Deletion of ORM2 causes oleic acid-induced growth defects in *Saccharomyces cerevisiae*. - *Appl Biochem Biotechnol* 195(10): 5916-5932.
- [22] Mbuyane, L. L., Bauer, F. F., Divol, B. (2021): The metabolism of lipids in yeasts and applications in oenology. - *Food Res Int* 141: 110142.
- [23] Monsalve-Atencio, R., Montano, D. F., Contreras-Calderon, J. (2023): Molecular imprinting technology and poly (ionic liquid)s: promising tools with industrial application for the removal of acrylamide and furanic compounds from coffee and other foods. - *Crit Rev Food Sci Nutr* 63(24): 6820-6839.
- [24] Otsu, M., Toume, M., Yamaguchi, Y., Tani, M. (2020): Proper regulation of inositolphosphorylceramide levels is required for acquirement of low pH resistance in budding yeast. - *Sci Rep* 10(1): 10792.
- [25] Park, S. H., Jo, A., Lee, K. G. (2021): Effect of various roasting, extraction and drinking conditions on furan and 5-hydroxymethylfurfural levels in coffee. - *Food Chem* 358: 129806.
- [26] Peng, D., Ruan, C., Fu, S., He, C., Song, J., Li, H., Tu, Y., Tang, D., Yao, L., Lin, S., Shi, Y., Zhang, W., Zhou, H., Zhu, L., Ma, C., Chang, C., Ma, J., Xie, Z., Wang, C., Xue, Y. (2021): Atg9-centered multi-omics integration reveals new autophagy regulators in *Saccharomyces cerevisiae*. - *Autophagy* 17(12): 4453-4476.
- [27] ,Ran, H., Zhang, J., Gao, Q., Lin, Z., Bao, J. (2014): Analysis of biodegradation performance of furfural and 5-hydroxymethylfurfural by *Amorphotheca resinae* ZN1. - *Biotechnol Biofuels* 7(1): 51.
- [28] Ruiz, M., Devkota, R., Kaper, D., Ruhanen, H., Busayavalasa, K., Radovic, U., Henricsson, M., Kakela, R., Boren, J., Pilon, M. (2023): AdipoR2 recruits protein interactors to promote fatty acid elongation and membrane fluidity. - *J Biol Chem* 299(6): 104799.
- [29] Sachse, B., Meinl, W., Sommer, Y., Glatt, H., Seidel, A., Monien, B. H. (2016): Bioactivation of food genotoxicants 5-hydroxymethylfurfural and furfuryl alcohol by sulfotransferases from human, mouse and rat: a comparative study. - *Arch Toxicol* 90(1): 137-148.
- [30] Salis, S., Spano, N., Ciulu, M., Floris, I., Pilo, M. I., Sanna, G. (2021): Electrochemical determination of the “furanic index” in honey. - *Molecules* 26(14).
- [31] Santos, A. A., Kretzer, L. G., Dourado, E. D. R., Rosa, C. A., Stambuk, B. U., Alves, S. L. (2025): Expression of a periplasmic beta-glucosidase from *Yarrowia lipolytica* allows efficient cellobiose-xylose co-fermentation by industrial xylose-fermenting *Saccharomyces cerevisiae* strains. - *Braz J Microbiol* 56(1): 91-104.
- [32] Sastre, D. E., Basso, L. G. M., Trastoy, B., Cifuentes, J. O., Contreras, X. F. Gueiros-Filho, de Mendoza, D., Navarro, M., Guerin, M. E. (2020): Membrane fluidity adjusts the insertion of the transacylase PlsX to regulate phospholipid biosynthesis in Gram-positive bacteria. - *J Biol Chem* 295(7): 2136-2147.
- [33] Seidel, T. (2022): The plant V-ATPase. - *Front Plant Sci* 13: 931777.
- [34] Shannon, P., Markiel, A., Ozier, O., Baliga, N. S. Wang, J. T., Ramage, D., Amin, N., Schwikowski, B., Ideker, T. (2003): Cytoscape: a software environment for integrated models of biomolecular interaction networks. - *Genome Res* 13(11): 2498-2504.
- [35] Shapla, U. M., Solayman, M., Alam, N., Khalil, M. I. Gan, S. H. (2018): 5-Hydroxymethylfurfural (HMF) levels in honey and other food products: effects on bees and human health. - *Chem Cent J* 12(1): 35.

- [36] Soares, C., Bergmann, J. C., de Almeida, J. R. M. (2021): Variable and dose-dependent response of *Saccharomyces* and non-*Saccharomyces* yeasts toward lignocellulosic hydrolysate inhibitors. - *Braz J Microbiol* 52(2): 575-586.
- [37] Sun, Y., Wang, X., Yang, X., Wang, L., Ding, J., Wang, C. C., Zhang, H., Wang, X. (2023): V-ATPase recruitment to ER exit sites switches COPII-mediated transport to lysosomal degradation. - *Dev Cell* 58(23): 2761-2775 e2765.
- [38] Tanaka, S., Tani, M. (2018): Mannosylinositol phosphorylceramides and ergosterol coordinately maintain cell wall integrity in the yeast *Saccharomyces cerevisiae*. - *FEBS J* 285(13): 2405-2427.
- [39] Tani, M., Toume, M. (2015): Alteration of complex sphingolipid composition and its physiological significance in yeast *Saccharomyces cerevisiae* lacking vacuolar ATPase. - *Microbiology (Reading)* 161(12): 2369-2383.
- [40] Vina-Gonzalez, J., Martinez, A. T., Guallar, V., Alcalde, M. (2020): Sequential oxidation of 5-hydroxymethylfurfural to furan-2,5-dicarboxylic acid by an evolved aryl-alcohol oxidase. - *Biochim Biophys Acta Proteins Proteom* 1868(1): 140293.
- [41] Wang, D., Hao, L., Jiao, X., Que, Z., Huang, J., Jin, Y., Zhou, R., Wang, Z., Wu, C. (2024): Engineering the synthesis of unsaturated fatty acids by introducing desaturase improved the stress tolerance of yeast. - *J Sci Food Agric* 104(4): 2398-2405.
- [42] Wang, H., Li, Q., Zhang, Z., Ayepa, E., Xiang, Q., Yu, X., Zhao, K., Zou, L., Gu, Y., Li, X., Chen, Q., Zhang, X., Yang, Y., Jin, X., Yin, H., Liu, Z. L., Tang, T., Liu, B., Ma, M. (2023): Discovery of new strains for furfural degradation using adaptive laboratory evolution in *Saccharomyces cerevisiae*. - *J Hazard Mater* 459: 132090.
- [43] Wu, D., Wang, D., Hong, J. (2020): Effect of a novel alpha/beta hydrolase domain protein on tolerance of *K. marxianus* to lignocellulosic biomass derived inhibitors. - *Front Bioeng Biotechnol* 8: 844.
- [44] Xu, T., Xia, R., He, F., Dong, E. H., Shen, J. M., Xu, C. C., Ji, M. H., Xu, Q., (2023): 5-Hydroxymethylfurfural induces mice frailty through cell senescence-associated sarcopenia caused by chronic inflammation. - *Heliyon* 9(2): e13217.
- [45] Zhuang, T., Gao, C., Zeng, W., Zhao, W., Yu, H., Chen, S., Shen, J., Ji, M. (2025): Analysis of key targets for 5-hydroxymethyl-2-furfural-induced lung cancer based on network toxicology, network informatics, and in vitro experiments. - *Drug Chem Toxicol* 48(2): 451-461.

APPENDIX

Table A1. The scores of each knockout strain analyzed by SGAtool under HMF conditions

No	Array ORF	Array name	Normalized colony size (EXPERIMENT)	Normalized colony std. dev. (EXPERIMENT)	Normalized colony size (CONTROL)	Normalized colony std. dev. (CONTROL)	Score	Score st dev	p-Value	Note
1	YMR283C	RIT1	0.38	0.01	1.04	0.03	-0.66	0.01	0	ss
2	YDR049W	VMS1	0.38	0	0.98	0.02	-0.6	0	0	ss
3	YJR075W	HOC1	0.69	0.01	1.21	0.02	-0.52	0.01	0	ss
4	YBL047C	EDE1	0.4	0.02	0.92	0.01	-0.52	0.02	0	ss
5	YDR068W	DOS2	0.42	0.04	0.94	0.02	-0.52	0.04	0	ss
6	YGL105W	ARC1	0.27	0.01	0.78	0	-0.51	0.01	0	ss
7	YHR030C	SLT2	0.8	0.05	1.29	0.05	-0.48	0.05	0	ss
8	YOR191W	ULS1	0.65	0.02	1.11	0.03	-0.46	0.02	0	ss
9	YMR272C	SCS7	0.61	0.07	1.06	0.02	-0.45	0.07	0	ss
10	YJL124C	LSM1	0.43	0.02	0.88	0.03	-0.45	0.02	0	ss
11	YDR360W	YDR360W	0.62	0.02	1.05	0	-0.43	0.02	0	ss
12	YNL032W	SIW14	0.72	0.02	1.12	0.12	-0.42	0.02	0	ss
13	YML035C	AMD1	0.51	0.01	0.93	0.04	-0.41	0.01	0	ss
14	YBR025C	OLA1	0.55	0.01	0.96	0.01	-0.41	0.01	0	ss
15	YDR378C	LSM6	0.29	0.02	0.69	0.03	-0.4	0.02	0	ss
16	YNR051C	BRE5	0.64	0	1.05	0.02	-0.4	0	0	ss
17	YLR217W	YLR217W	0.94	0.02	1.35	0.03	-0.39	0.02	0	ss
18	YJL121C	RPE1	0.37	0.05	0.75	0.05	-0.39	0.05	0	ss
19	YMR275C	BUL1	0.66	0.03	1.02	0.04	-0.37	0.03	0	ss
20	YKL023W	YKL023W	0.64	0.04	1.01	0.03	-0.36	0.04	0	ss
21	YNR005C	YNR005C	0.74	0.01	1.09	0.06	-0.35	0.01	0	ss
22	YLR085C	ARP6	0.67	0	1.03	0.04	-0.34	0	0	ss
23	YML041C	VPS71	0.63	0.04	0.98	0.04	-0.34	0.04	0	ss
24	YJR059W	PTK2	0.49	0.04	0.83	0.02	-0.34	0.04	0	ss
25	YNL136W	EAF7	0.45	0.02	0.78	0.03	-0.33	0.02	0	ss
26	YJL136C	RPS21B	0.6	0.06	0.92	0.02	-0.32	0.06	0	ss

No	Array ORF	Array name	Normalized colony size (EXPERIMENT)	Normalized colony std. dev. (EXPERIMENT)	Normalized colony size (CONTROL)	Normalized colony std. dev. (CONTROL)	Score	Score st dev	p-Value	Note
27	YLR330W	CHS5	0.85	0.03	1.16	0.04	-0.32	0.03	0	ss
28	YCR053W	THR4	0.65	0.02	0.97	0.01	-0.31	0.02	0	ss
29	YNL099C	OCA1	0.78	0.01	1.09	0.03	-0.31	0.01	0	ss
30	YGL084C	GUP1	0.51	0.01	0.8	0.01	-0.3	0.01	0	ss
31	YDL078C	MDH3	0.91	0.03	1.21	0.04	-0.3	0.03	0	ss
32	YOR006C	TSR3	0.86	0.05	1.16	0.06	-0.3	0.05	0	ss
33	YDR067C	OCA6	0.73	0.02	1.03	0.03	-0.3	0.02	0	ss
34	YER151C	UBP3	0.73	0.01	1.02	0.01	-0.29	0.01	0	ss
35	YNL229C	URE2	0.69	0.02	0.98	0.01	-0.29	0.02	0	ss
36	YPR134W	MSS18	0.55	0.02	0.84	0	-0.29	0.02	0	ss
37	YPR024W	YME1	0.56	0.01	0.84	0.02	-0.28	0.01	0	ss
38	YKL046C	DCW1	0.94	0.09	1.22	0.05	-0.28	0.09	0	ss
39	YHR086W	NAM8	0.75	0.04	1.02	0.03	-0.28	0.04	0	ss
40	YDL050C	YDL050C	0.74	0	1.01	0.01	-0.27	0	0	ss
41	YML008C	ERG6	0.5	0.02	0.77	0.02	-0.27	0.02	0	ss
42	YNL147W	LSM7	0.51	0.05	0.78	0.04	-0.27	0.05	0	ss
43	YGR038W	ORM1	0.93	0.01	1.2	0.03	-0.26	0.01	0	ss
44	YNL254C	RTC4	0.82	0.05	1.08	0.02	-0.26	0.05	0	ss
45	YPL183C	RTT10	0.73	0	0.99	0.02	-0.26	0	0	ss
46	YMR026C	PEX12	0.78	0.03	1.02	0.05	-0.25	0.03	0	ss
47	YBL094C	YBL094C	0.71	0.01	0.96	0.07	-0.25	0.01	0	ss
48	YDR485C	VPS72	0.67	0.01	0.92	0	-0.25	0.01	0	ss
49	YJL062W	LAS21	0.74	0.02	0.99	0.01	-0.25	0.02	0	ss
50	YOR012W	YOR012W	0.76	0.02	1	0.01	-0.25	0.02	0	ss
51	YHR078W	YHR078W	0.85	0.03	1.09	0.01	-0.24	0.03	0	ss
52	YNL008C	ASI3	0.95	0.03	1.19	0.05	-0.24	0.03	0	ss
53	YFL023W	BUD27	0.64	0.03	0.88	0.03	-0.24	0.03	0	ss
54	YJR082C	EAF6	0.78	0.02	1.02	0.02	-0.24	0.02	0	ss
55	YNL072W	RNH201	0.76	0.03	1	0.02	-0.24	0.03	0	ss
56	YMR282C	AEP2	0.78	0.02	1.01	0.04	-0.23	0.02	0	ss
57	YLR452C	SST2	0.99	0.02	1.23	0.02	-0.23	0.02	0	ss
58	YBR001C	NTH2	0.74	0.02	0.97	0	-0.23	0.02	0	ss
59	YNL089C	YNL089C	0.85	0.02	1.08	0.02	-0.23	0.02	0	ss

No	Array ORF	Array name	Normalized colony size (EXPERIMENT)	Normalized colony std. dev. (EXPERIMENT)	Normalized colony size (CONTROL)	Normalized colony std. dev. (CONTROL)	Score	Score st dev	p-Value	Note
60	YMR031W-A	YMR031W-A	0.59	0.03	0.83	0.03	-0.23	0.03	0	ss
61	YLR332W	MID2	0.92	0.05	1.14	0.04	-0.23	0.05	0	ss
62	YHR066W	SSF1	0.77	0.01	1	0.01	-0.23	0.01	0	ss
63	YBL007C	SLA1	0.64	0.01	0.87	0.03	-0.23	0.01	0	ss
64	YJR074W	MOG1	0.64	0.05	0.87	0.03	-0.23	0.05	0	ss
65	YDR304C	CPR5	0.88	0.01	1.11	0.03	-0.23	0.01	0	ss
66	YLR098C	CHA4	0.89	0.01	1.12	0.04	-0.23	0.01	0	ss
67	YIL132C	CSM2	0.91	0.07	1.13	0.03	-0.22	0.07	0	ss
68	YLR070C	XYL2	0.94	0.06	1.17	0.05	-0.22	0.06	0	ss
69	YMR318C	ADH6	0.81	0.02	1.03	0.02	-0.22	0.02	0	ss
70	YDR532C	KRE28	0.57	0.01	0.79	0.02	-0.22	0.01	0	ss
71	YJR097W	JJ3	0.7	0.03	0.93	0.03	-0.22	0.03	0	ss
72	YJL211C	YJL211C	0.89	0.04	1.1	0.05	-0.22	0.04	0	ss
73	YGR051C	YGR051C	0.97	0.02	1.19	0.11	-0.22	0.02	0	ss
74	YFL013C	IES1	0.87	0.03	1.09	0.05	-0.22	0.03	0	ss
75	YDR334W	SWR1	0.72	0.01	0.94	0.03	-0.22	0.01	0	ss
76	YHR110W	ERP5	0.9	0.02	1.12	0	-0.22	0.02	0	ss
77	YHL024W	RIM4	0.92	0.01	1.13	0.01	-0.21	0.01	0	ss
78	YGR055W	MUP1	0.62	0.02	0.84	0.04	-0.21	0.02	0	ss
79	YCL009C	ILV6	0.94	0.04	1.15	0.04	-0.21	0.04	0	ss
80	YLL046C	RNP1	0.98	0	1.21	0.1	-0.21	0	0	ss
81	YCR085W	YCR085W	0.81	0.02	1.01	0.02	-0.21	0.02	0	ss
82	YHL023C	NPR3	0.83	0.01	1.04	0.03	-0.21	0.01	0	ss
83	YJL141C	YAK1	0.84	0.1	1.04	0.03	-0.21	0.1	0	ss
84	YCR062W	YCR062W	0.86	0.03	1.08	0.03	-0.21	0.03	0	ss
85	YPL213W	LEA1	0.67	0.01	0.88	0.02	-0.2	0.01	0	ss
86	YGL059W	PKP2	0.97	0.04	1.18	0.01	-0.2	0.04	0	ss
87	YBL024W	NCL1	0.77	0.02	0.97	0	-0.2	0.02	0	ss
88	YKR084C	HBS1	0.67	0.03	0.88	0.02	-0.2	0.03	0	ss
89	YPL105C	SYH1	0.89	0.01	1.09	0.01	-0.2	0.01	0	ss
90	YGR122C-A	YGR122C-A	0.98	0.02	1.19	0.04	-0.2	0.02	0	ss
91	YDL051W	LHP1	0.8	0.02	1	0.01	-0.2	0.02	0	ss
92	YMR163C	INP2	0.81	0.01	1.01	0.02	-0.2	0.01	0	ss

No	Array ORF	Array name	Normalized colony size (EXPERIMENT)	Normalized colony std. dev. (EXPERIMENT)	Normalized colony size (CONTROL)	Normalized colony std. dev. (CONTROL)	Score	Score st dev	p-Value	Note
93	YDL091C	UBX3	1.21	0.03	1.01	0.01	0.2	0.03	0	st
94	YKR019C	IRS4	1.19	0.05	0.99	0.01	0.2	0.05	0	st
95	YGL014W	PUF4	1.24	0.05	1.04	0.01	0.2	0.05	0	st
96	YOR108W	LEU9	1.15	0.05	0.94	0.01	0.2	0.05	0	st
97	YDR032C	PST2	1.17	0.03	0.97	0.02	0.2	0.03	0	st
98	YJR014W	TMA22	1.11	0.01	0.9	0.02	0.2	0.01	0	st
99	YOL081W	IRA2	1.03	0.08	0.82	0.02	0.2	0.08	0	st
100	YIL085C	KTR7	1.03	0.01	0.83	0.01	0.2	0.01	0	st
101	YER066W	RRT13	1.17	0.05	0.97	0.01	0.2	0.05	0	st
102	YGR183C	QCR9	1.07	0.01	0.86	0.04	0.2	0.01	0	st
103	YGL180W	ATG1	1.22	0.06	1.01	0.03	0.21	0.06	0	st
104	YLR177W	YLR177W	1.14	0.01	0.93	0.02	0.21	0.01	0	st
105	YCR009C	RVS161	1.05	0.03	0.84	0.01	0.21	0.03	0	st
106	YKR031C	SPO14	1.23	0.02	1.02	0	0.21	0.02	0	st
107	YML026C	RPS18B	1.04	0.02	0.84	0.02	0.21	0.02	0	st
108	YLR407W	YLR407W	1.08	0	0.87	0.03	0.21	0	0	st
109	YJR010C-A	SPC1	1.24	0.06	1.03	0.01	0.22	0.06	0	st
110	YBL104C	SEA4	1.11	0.01	0.89	0.01	0.22	0.01	0	st
111	YDL232W	OST4	0.91	0.05	0.7	0.01	0.22	0.05	0	st
112	YIL138C	TPM2	1.27	0.02	1.06	0.03	0.22	0.02	0	st
113	YGR105W	VMA21	1.04	0.02	0.83	0.02	0.22	0.02	0	st
114	YGR161C	RTS3	1.12	0.01	0.9	0.01	0.22	0.01	0	st
115	YBR141C	YBR141C	1.19	0.01	0.97	0.01	0.22	0.01	0	st
116	YKL146W	AVT3	1.15	0.02	0.94	0.02	0.22	0.02	0	st
117	YLR179C	YLR179C	1.26	0.04	1.05	0.04	0.22	0.04	0	st
118	YBR082C	UBC4	1.14	0.02	0.92	0.01	0.22	0.02	0	st
119	YEL057C	YEL057C	1.16	0.02	0.94	0.01	0.22	0.02	0	st
120	YCL036W	GFD2	1.2	0.04	0.98	0.01	0.22	0.04	0	st
121	YDR209C	YDR209C	1.3	0.01	1.08	0.03	0.22	0.01	0	st
122	YKL073W	LHS1	0.97	0.23	0.72	0.15	0.22	0.23	0	st
123	YKL048C	ELM1	0.92	0.06	0.7	0.02	0.22	0.06	0	st
124	YML004C	GLO1	1.21	0.01	0.98	0.01	0.22	0.01	0	st
125	YLR371W	ROM2	1.15	0.04	0.93	0.01	0.22	0.04	0	st

No	Array ORF	Array name	Normalized colony size (EXPERIMENT)	Normalized colony std. dev. (EXPERIMENT)	Normalized colony size (CONTROL)	Normalized colony std. dev. (CONTROL)	Score	Score st dev	p-Value	Note
126	YOR183W	FYV12	1.1	0.01	0.87	0.01	0.23	0.01	0	st
127	YLR176C	RFX1	1.27	0.03	1.05	0.01	0.23	0.03	0	st
128	YAL022C	FUN26	1.17	0.09	0.92	0.07	0.23	0.09	0	st
129	YKR020W	VPS51	1.28	0.03	1.05	0.01	0.23	0.03	0	st
130	YHR162W	MPC2	1.02	0.04	0.79	0.02	0.23	0.04	0	st
131	YKL174C	TPO5	1.21	0.03	0.98	0.02	0.23	0.03	0	st
132	YLR384C	IKI3	1.1	0.02	0.87	0	0.23	0.02	0	st
133	YOR193W	PEX27	1.18	0.01	0.95	0.01	0.23	0.01	0	st
134	YNL171C	YNL171C	1.05	0.01	0.82	0.02	0.23	0.01	0	st
135	YDR508C	GNP1	1.26	0.02	1.03	0.01	0.23	0.02	0	st
136	YPR018W	RLF2	1.12	0.04	0.89	0.02	0.23	0.04	0	st
137	YIR019C	FLO11	1.25	0.1	1.03	0.04	0.23	0.1	0	st
138	YLR443W	ECM7	1.14	0	0.92	0.03	0.23	0	0	st
139	YNL170W	YNL170W	0.9	0.03	0.66	0.02	0.23	0.03	0	st
140	YML097C	VPS9	1.17	0.01	0.93	0.02	0.23	0.01	0	st
141	YGR078C	PAC10	1.1	0.03	0.88	0.05	0.23	0.03	0	st
142	YOR182C	RPS30B	1.12	0.01	0.88	0.01	0.23	0.01	0	st
143	YMR145C	NDE1	1.23	0.07	0.99	0.02	0.23	0.07	0	st
144	YDL076C	RXT3	1.19	0	0.96	0.04	0.24	0	0	st
145	YKR047W	YKR047W	1.22	0.02	0.97	0.04	0.24	0.02	0	st
146	YMR029C	FAR8	1.19	0.04	0.96	0.02	0.24	0.04	0	st
147	YBR095C	RXT2	1.11	0.02	0.87	0	0.24	0.02	0	st
148	YNR029C	YNR029C	1.1	0.01	0.86	0.04	0.24	0.01	0	st
149	YMR271C	URA10	1.21	0.07	0.96	0.04	0.24	0.07	0	st
150	YLR327C	TMA10	1.16	0.03	0.91	0.03	0.24	0.03	0	st
151	YGL149W	YGL149W	1.21	0.02	0.98	0.02	0.24	0.02	0	st
152	YKL164C	PIR1	1.16	0.06	0.93	0.05	0.24	0.06	0	st
153	YML128C	MSC1	1.24	0.02	1	0.02	0.24	0.02	0	st
154	YDR156W	RPA14	1.34	0.03	1.1	0.03	0.24	0.03	0	st
155	YDL074C	BRE1	0.97	0	0.73	0.03	0.24	0	0	st
156	YMR039C	SUB1	1.28	0.08	1.04	0.02	0.24	0.08	0	st
157	YBR105C	VID24	0.95	0.01	0.71	0	0.24	0.01	0	st
158	YPL086C	ELP3	1.04	0.04	0.8	0	0.25	0.04	0	st

No	Array ORF	Array name	Normalized colony size (EXPERIMENT)	Normalized colony std. dev. (EXPERIMENT)	Normalized colony size (CONTROL)	Normalized colony std. dev. (CONTROL)	Score	Score st dev	p-Value	Note
159	YDR469W	SDC1	1.09	0.01	0.85	0.01	0.25	0.01	0	st
160	YKL092C	BUD2	1.2	0.03	0.95	0.01	0.25	0.03	0	st
161	YPL071C	YPL071C	1.04	0.02	0.8	0.01	0.25	0.02	0	st
162	YLR287C-A	RPS30A	1.17	0.04	0.92	0.03	0.25	0.04	0	st
163	YOR078W	BUD21	1.04	0.01	0.79	0.01	0.25	0.01	0	st
164	YBR181C	RPS6B	1.18	0	0.93	0.01	0.25	0	0	st
165	YKR023W	YKR023W	1.21	0.01	0.97	0.01	0.25	0.01	0	st
166	YLR015W	BRE2	1.16	0.03	0.91	0	0.25	0.03	0	st
167	YMR312W	ELP6	1.07	0.02	0.82	0.02	0.25	0.02	0	st
168	YMR152W	YIM1	1.16	0.05	0.91	0.01	0.25	0.05	0	st
169	YGL179C	TOS3	1.22	0.02	0.97	0.01	0.25	0.02	0	st
170	YFL030W	AGX1	1.12	0.03	0.86	0.03	0.26	0.03	0	st
171	YKL109W	HAP4	1.11	0.05	0.86	0.01	0.26	0.05	0	st
172	YHR200W	RPN10	1.16	0.06	0.9	0.01	0.26	0.06	0	st
173	YIL154C	IMP2*	1.23	0.01	0.97	0.01	0.26	0.01	0	st
174	YLR024C	UBR2	1.21	0.04	0.95	0.03	0.26	0.04	0	st
175	YNL224C	SQS1	1.19	0.02	0.93	0.03	0.26	0.02	0	st
176	YML035C-A	YML035C-A	1.24	0.02	0.98	0.02	0.26	0.02	0	st
177	YHR194W	MDM31	0.93	0.01	0.67	0.02	0.26	0.01	0	st
178	YDR459C	PFA5	1.14	0.02	0.88	0.04	0.26	0.02	0	st
179	YMR067C	UBX4	1.08	0.04	0.82	0.02	0.26	0.04	0	st
180	YLR320W	MMS22	1.07	0.01	0.81	0.01	0.26	0.01	0	st
181	YDR466W	PKH3	1.17	0.01	0.91	0.02	0.26	0.01	0	st
182	YHR059W	FYV4	1.02	0.05	0.76	0.01	0.26	0.05	0	st
183	YDL189W	RBS1	1.26	0.01	1	0.03	0.26	0.01	0	st
184	YDR096W	GIS1	1.33	0.01	1.07	0.03	0.26	0.01	0	st
185	YIL141W	YIL141W	1.26	0.01	0.99	0.03	0.26	0.01	0	st
186	YPL196W	OXR1	1.25	0.02	0.98	0.03	0.26	0.02	0	st
187	YML051W	GAL80	1.25	0.08	0.98	0.05	0.26	0.08	0	st
188	YHR096C	HXT5	1.32	0.04	1.06	0.01	0.27	0.04	0	st
189	YMR223W	UBP8	1.27	0	1	0.02	0.27	0	0	st
190	YGR200C	ELP2	1.04	0	0.76	0.03	0.27	0	0	st
191	YGL250W	RMR1	1.27	0.03	1	0	0.27	0.03	0	st

No	Array ORF	Array name	Normalized colony size (EXPERIMENT)	Normalized colony std. dev. (EXPERIMENT)	Normalized colony size (CONTROL)	Normalized colony std. dev. (CONTROL)	Score	Score st dev	p-Value	Note
192	YJL169W	YJL169W	1.12	0.06	0.85	0.03	0.27	0.06	0	st
193	YDR517W	GRH1	1.22	0.01	0.95	0.02	0.27	0.01	0	st
194	YJR108W	ABM1	1.22	0.06	0.95	0.01	0.27	0.06	0	st
195	YPR132W	RPS23B	1.16	0.03	0.9	0.02	0.27	0.03	0	st
196	YDR374C	YDR374C	1.03	0.01	0.76	0.02	0.27	0.01	0	st
197	YKL026C	GPX1	1.14	0.05	0.86	0.01	0.27	0.05	0	st
198	YNL319W	YNL319W	1.07	0.07	0.8	0.03	0.28	0.07	0	st
199	YBR189W	RPS9B	1.15	0.01	0.88	0.02	0.28	0.01	0	st
200	YPL181W	CTI6	1.27	0.05	0.99	0.03	0.28	0.05	0	st
201	YIL077C	YIL077C	1.18	0.04	0.89	0	0.28	0.04	0	st
202	YKL179C	COY1	1.24	0.01	0.96	0.03	0.28	0.01	0	st
203	YNR064C	YNR064C	1.22	0.09	0.95	0.04	0.28	0.09	0	st
204	YPR151C	SUE1	1.2	0.04	0.92	0.02	0.29	0.04	0	st
205	YGL181W	GTS1	1.2	0.11	0.91	0.09	0.29	0.11	0	st
206	YOL053W	AIM39	1.02	0.05	0.73	0.05	0.29	0.05	0	st
207	YMR315W	YMR315W	1.2	0.04	0.9	0.01	0.29	0.04	0	st
208	YLR264W	RPS28B	1.15	0.03	0.86	0.02	0.29	0.03	0	st
209	YGL244W	RTF1	0.93	0.02	0.63	0.03	0.29	0.02	0	st
210	YMR100W	MUB1	1.15	0.03	0.87	0.04	0.3	0.03	0	st
211	YJR011C	YJR011C	1.03	0.01	0.74	0.01	0.3	0.01	0	st
212	YLR172C	DPH5	1.09	0.06	0.79	0	0.3	0.06	0	st
213	YML102W	CAC2	1.27	0.02	0.97	0.01	0.3	0.02	0	st
214	YGR239C	PEX21	1.17	0.05	0.87	0.02	0.3	0.05	0	st
215	YOL007C	CSI2	1.26	0	0.96	0.02	0.3	0	0	st
216	YKR074W	AIM29	1.28	0.02	0.97	0.02	0.3	0.02	0	st
217	YMR219W	ESC1	1.32	0.05	1.02	0.02	0.3	0.05	0	st
218	YDR458C	HEH2	1.22	0.08	0.91	0.01	0.3	0.08	0	st
219	YOR139C	YOR139C	1.28	0	0.97	0	0.3	0	0	st
220	YHR111W	UBA4	1.21	0.02	0.9	0.02	0.31	0.02	0	st
221	YBR275C	RIF1	1.38	0	1.07	0.02	0.31	0	0	st
222	YDL093W	PMT5	1.18	0.02	0.87	0.02	0.31	0.02	0	st
223	YER067C-A	YER067C-A	1.18	0.05	0.86	0.01	0.32	0.05	0	st
224	YOL059W	GPD2	1.23	0.02	0.92	0.04	0.32	0.02	0	st

No	Array ORF	Array name	Normalized colony size (EXPERIMENT)	Normalized colony std. dev. (EXPERIMENT)	Normalized colony size (CONTROL)	Normalized colony std. dev. (CONTROL)	Score	Score st dev	p-Value	Note
225	YKR103W	NFT1	1.32	0.03	1	0	0.32	0.03	0	st
226	YIL153W	RRD1	1.28	0.04	0.96	0.02	0.32	0.04	0	st
227	YOL080C	REX4	1.33	0.01	1.01	0.01	0.32	0.01	0	st
228	YDL187C	YDL187C	1.28	0.03	0.96	0.02	0.32	0.03	0	st
229	YLR004C	THI73	1.23	0.03	0.91	0.02	0.32	0.03	0	st
230	YHR034C	PIH1	1.18	0.04	0.85	0.01	0.33	0.04	0	st
231	YLR412W	BER1	1.14	0.01	0.82	0.01	0.33	0.01	0	st
232	YBR009C	HHF1	1.25	0.08	0.92	0.03	0.33	0.08	0	st
233	YJR058C	APS2	1.2	0.01	0.87	0.01	0.33	0.01	0	st
234	YLR131C	ACE2	1.27	0.03	0.93	0	0.33	0.03	0	st
235	YOR301W	RAX1	1.2	0.02	0.86	0.01	0.34	0.02	0	st
236	YNL206C	RTT106	1.19	0.01	0.86	0.01	0.34	0.01	0	st
237	YDL083C	RPS16B	1.19	0.03	0.85	0.02	0.34	0.03	0	st
238	YNL045W	LAP2	1.2	0.03	0.86	0	0.34	0.03	0	st
239	YDR313C	PIB1	1.3	0.01	0.95	0.01	0.35	0.01	0	st
240	YBR095C	RXT2	1.31	0.01	0.97	0.01	0.35	0.01	0	st
241	YJR087W	YJR087W	1.38	0.12	1.03	0.03	0.35	0.12	0	st
242	YDR257C	RKM4	1.34	0.06	0.98	0.04	0.35	0.06	0	st
243	YDL129W	YDL129W	1.44	0.03	1.08	0.01	0.36	0.03	0	st
244	YOR089C	VPS21	1.29	0.02	0.93	0.01	0.36	0.02	0	st
245	YOR135C	YOR135C	0.97	0.04	0.61	0.02	0.36	0.04	0	st
246	YLR423C	ATG17	1.29	0.01	0.92	0.05	0.36	0.01	0	st
247	YOR045W	TOM6	1.3	0.02	0.94	0.01	0.36	0.02	0	st
248	YBR082C	UBC4	1.29	0.03	0.91	0.03	0.37	0.03	0	st
249	YKL213C	DOA1	1.26	0.03	0.89	0.01	0.37	0.03	0	st
250	YLR418C	CDC73	0.92	0.02	0.55	0.02	0.37	0.02	0	st
251	YPL032C	SVL3	1.16	0.03	0.79	0.03	0.37	0.03	0	st
252	YPL139C	UME1	1.28	0.03	0.91	0.01	0.37	0.03	0	st
253	YMR252C	YMR252C	1.21	0.03	0.83	0.01	0.37	0.03	0	st
254	YLR048W	RPS0B	1.15	0.03	0.77	0.01	0.38	0.03	0	st
255	YMR124W	YMR124W	1.2	0	0.82	0.02	0.38	0	0	st
256	YMR274C	RCE1	1.29	0.05	0.91	0.01	0.38	0.05	0	st
257	YLR174W	IDP2	1.34	0.05	0.94	0.03	0.39	0.05	0	st

No	Array ORF	Array name	Normalized colony size (EXPERIMENT)	Normalized colony std. dev. (EXPERIMENT)	Normalized colony size (CONTROL)	Normalized colony std. dev. (CONTROL)	Score	Score st dev	p-Value	Note
258	YLR388W	RPS29A	1.2	0.03	0.81	0	0.39	0.03	0	st
259	YAR002W	NUP60	1.32	0.01	0.93	0.01	0.39	0.01	0	st
260	YHR048W	YHK8	1.33	0.05	0.93	0.04	0.4	0.05	0	st
261	YOR007C	SGT2	1.14	0.03	0.73	0	0.4	0.03	0	st
262	YMR073C	IRC21	1.27	0.01	0.87	0.01	0.41	0.01	0	st
263	YMR025W	CSII	1.44	0.09	1.02	0.03	0.41	0.09	0	st
264	YOL103W	ITR2	1.17	0.05	0.75	0.02	0.42	0.05	0	st
265	YIL008W	URM1	1.31	0.06	0.85	0.04	0.45	0.06	0	st
266	YML048W-A	YML048W-A	1.24	0.04	0.79	0.03	0.45	0.04	0	st
267	YML010C-B	YML010C-B	1.37	0.08	0.92	0.01	0.46	0.08	0	st
268	YKL066W	YKL066W	1.47	0.01	1	0.02	0.47	0.01	0	st
269	YKR072C	SIS2	1.43	0.04	0.97	0.01	0.47	0.04	0	st
270	YLR218C	COA4	1.35	0.06	0.88	0.02	0.48	0.06	0	st
271	YOR312C	RPL20B	1.46	0.11	0.97	0.01	0.48	0.11	0	st
272	YML102C-A	YML102C-A	1.31	0.02	0.83	0.01	0.48	0.02	0	st
273	YMR105C	PGM2	1.45	0.01	0.96	0.03	0.49	0.01	0	st
274	YOL068C	HST1	1.35	0.02	0.87	0.03	0.49	0.02	0	st
275	YKL037W	AIM26	1.12	0.02	0.62	0	0.5	0.02	0	st
276	YHR003C	YHR003C	1.42	0.02	0.92	0.01	0.5	0.02	0	st
277	YKL074C	MUD2	1.41	0.01	0.9	0.03	0.5	0.01	0	st
278	YIL108W	YIL108W	1.41	0.05	0.91	0.04	0.5	0.05	0	st
279	YCR063W	BUD31	1.26	0.01	0.75	0.03	0.51	0.01	0	st
280	YGR201C	YGR201C	1.55	0.04	1.04	0.03	0.51	0.04	0	st
281	YGR170W	PSD2	1.29	0.04	0.77	0.05	0.53	0.04	0	st
282	YCL037C	SRO9	1.37	0.01	0.82	0.01	0.55	0.01	0	st
283	YAL013W	DEP1	1.36	0.09	0.8	0.02	0.57	0.09	0	st
284	YDR348C	PAL1	1.55	0.02	0.98	0.01	0.57	0.02	0	st
285	YGR202C	PCT1	1.51	0.04	0.94	0.03	0.58	0.04	0	st
286	YNL040W	YNL040W	1.58	0.05	1	0.03	0.59	0.05	0	st
287	YPL182C	YPL182C	1.61	0.07	1.01	0.02	0.59	0.07	0	st
288	YJL016W	YJL016W	1.44	0.04	0.84	0.02	0.6	0.04	0	st
289	YKL015W	PUT3	1.58	0.15	0.95	0.01	0.63	0.15	0	st
290	YKL076C	YKL076C	1.54	0.06	0.9	0.01	0.64	0.06	0	st

No	Array ORF	Array name	Normalized colony size (EXPERIMENT)	Normalized colony std. dev. (EXPERIMENT)	Normalized colony size (CONTROL)	Normalized colony std. dev. (CONTROL)	Score	Score st dev	p-Value	Note
291	YOL004W	SIN3	1.39	0.02	0.73	0.01	0.66	0.02	0	st
292	YKL069W	YKL069W	1.36	0.02	0.7	0.01	0.66	0.02	0	st
293	YKR082W	NUP133	1.37	0.02	0.68	0.02	0.68	0.02	0	st
294	YMR106C	YKU80	1.69	0	0.96	0.02	0.74	0	0	st

Below - 0.2 is significantly sensitive (ss), and 0.2 is tolerant (st)